J. Membrane Biol. 171, 63–73 (1999)

The Journal of
Membrane
Biology

Transport Systems of *Ventricaria ventricosa: I/V* Analysis of Both Membranes in Series as a Function of $[K^+]_o$

M.J. Beilby[1], **M.A. Bisson**[2]

[1]Biophysics Department, School of Physics, University of New South Wales, Sydney 2052, Australia
[2]Department of Biological Sciences, State University of New York at Buffalo, Cooke Hall 109, Box 1300, Buffalo, NY 14260-1300, USA

Received: 5 November 1998/Revised: 11 May 1999

Abstract. The current-voltage (*I/V*) profiles of *Ventricaria* (formerly *Valonia*) membranes were measured at a range of external potassium concentrations, $[K^+]_o$, from 0.1 to 100 mM. The conductance-voltage (*G/V*) characteristics were computed to facilitate better resolution of the profile change with time after exposure to different $[K^+]_o$. The resistance-voltage (*R/V*) characteristics were computed to attempt resolution of plasmalemma and tonoplast. Four basic electrophysiological stages emerged: (1) Uniform low resistance between −60 and +60 mV after the cell impalement. (2) High resistance between +50 and +150 for $[K^+]_o$ from 0.1 to 1.0 mM and hypotonic media. (3) High resistance between −150 and −20 mV for $[K^+]_o$ of 10 mM (close to natural seawater) and hypertonic media. (4) High resistance between −150 and +170 mV at $[K^+]_o$ of 100 mM.

The changes between these states were slow, requiring minutes to hours and sometimes exhibiting spontaneous oscillations of the membrane p.d. (potential difference). Our analysis of the *I/V* data supports a previous hypothesis, that *Ventricaria* tonoplast is the more resistive membrane containing a pump, which transports K^+ into the vacuole to regulate turgor. We associate state (1) with the plasmalemma conductance being dominant and the K^+ pump at the tonoplast short-circuited probably by a K^+ channel, state (2) with the K^+ pump "off" or short-circuited at p.d.s more negative than +50 mV, state (3) with the K^+ pump "on," and state (4) with the pump dominant, but affected by high K^+. A model for the *Ventricaria* membrane system is proposed.

Key words: *Ventricaria* (*Valonia*) — *I/V* analysis — Potassium dependence — Electrogenic pump — Turgor regulation

Correspondence to: M.J. Beilby

Introduction

Ventricaria (formerly *Valonia*—Olsen & West, 1988) is a marine alga comprised mostly of a single multinucleate cell, which may be several centimeters in diameter. Its large size has made it a convenient organism for the study of electrophysiology. Early experiments (Blinks, 1929) indicated a positive membrane potential, which is unusual, since most cells have negative membrane potentials. Damon (1930) first suggested that the cytoplasm is negative to the exterior, but the vacuole is positive to the cytoplasm, and the algebraic sum of the two potentials results in a positive electrical potential difference, when a microelectrode is inserted into the vacuole, as usually occurs when mature cells are impaled. This hypothesis was confirmed by Gutknecht using aplanospores, which form from the larger cells by dividing the cytoplasm into many small uninucleate cells lacking vacuoles for some hours after formation (Gutknecht, 1966). Gutknecht measured a negative membrane potential of about −71 mV, consistent with generation of the membrane potential by K^+ diffusion, since the equilibrium potential for K^+, E_K, is −92 mV. Assuming that the same is true of the mature *Ventricaria* cell, Gutknecht deduced that its vacuole must be about +88 mV positive to the cytoplasm, to give an overall vacuolar potential of about +17 mV. Final confirmation came from Davis (1981), who performed separate measurements of the p.d. across the tonoplast and the plasmalemma by impaling the cytoplasm in the mature cells. His measurements also suggest that the tonoplast resistance is 2 to 3 times greater than that of the plasmalemma. This feature is also unusual compared to most plant cells studied.

The measurements of ion concentrations from extracted vacuolar sap and cytoplasm and of isotopic fluxes of these ions allowed Gutknecht (1966) to infer the active and passive transport which must be occurring at

each membrane. Na^+ must be actively transported out of the cytoplasm at both membranes, while K^+ is close to equilibrium at the plasmalemma and is actively taken up into the vacuole across the tonoplast. Cl^- fluxes at both membranes can be accounted for by passive diffusion. More recent experiments (Wang, Benz & Zimmermann, 1995) indicate by indirect means that the activity of the Cl^- carrier may be linked to metabolic activity, but this does not necessarily contradict the thermodynamic conclusion that active transport is not necessary to generate the Cl^- fluxes measured. The pH of the cytoplasm has not been measured, but if it is close to 7, then H^+ approaches equilibrium with seawater of pH 8. The pH of the vacuole was measured as 6.9 in the dark (Davis, 1981) suggesting active transport of H^+ into the vacuole. Further acidification in the light to pH 5.8 (Davis, 1981) supports this view, linking the energy source with photosynthesis.

The inwardly directed tonoplast K^+ active transport has significance for the response of the cell to hypertonic stress. Gutknecht (1967) established that hypertonic stress stimulated an inward current under short-circuit conditions which was associated with a K^+ influx in a one-to-one ratio. Hastings and Gutknecht (1974, 1975) showed that the stimulation was due to changes in turgor pressure rather than other parameters of salt stress, and that the active K^+ influx at the tonoplast, presumably accompanied by passive K^+ influx at the plasma membrane and passive Cl^- influxes at both membranes, accounted for 85% of the regulatory increase in vacuolar sap osmotic pressure.

Ventricaria is not the only organism with such an unusual survival strategy. Related genera of class *Bryopsidophyceae*, *Valonia* sp. (Hastings & Gutknecht, 1975), *Chaetomorpha darwinii* (Findlay et al., 1971) and *Valoniopsis pachynema* (Findlay et al., 1978), also display positive vacuolar p.d. and *Chaetomorpha* exhibits tonoplast resistance an order of magnitude greater than that of the plasmalemma. The electrophysiology of these plant cells is, therefore, likely to reveal novel transporters or novel combinations of familiar transporters, as well as illuminating more conventional transport schemes. The *Ventricaria* cells also provide a convenient system to gain more insight into signal cascades involved in turgor regulation.

We report here new findings on ion transport in *Ventricaria*, using current-voltage (*I/V*) analysis to distinguish the passive K^+ transport at the plasma membrane and the active, stress-induced K^+ transport at the tonoplast.

Materials and Methods

Ventricaria ventricosa specimens were collected at Heron Island, Queensland, Australia, and transported to the laboratory at the University of New South Wales, where they were maintained in seawater from Heron Island or Coogee Beach in New South Wales. Data reported here were obtained from collected cells 2 to 3 mm in diameter.

During the experiments, cells were bathed in a simplified artificial seawater, ASW, comprised of (in mM): 450 NaCl, 10 KCl, 50 $MgSO_4$, 8 $CaCl_2$, buffered to pH 8.0 with 10 mM HEPES (4-2[hydroxyethyl]-1-piperazine-ethane sulfonic acid) and NaOH, osmotic pressure of 990 mOsm. Diminished K^+ concentrations were achieved by reducing the external KCl from 10 to 1 or 0.1. Changes of Cl^- concentration and osmotic pressure caused by this decrease were minimal. High K^+ concentration was produced by increasing the KCl concentration to 100 mM, while reducing the NaCl concentration by an equivalent amount. The hypertonic stress was achieved by increasing the NaCl concentration to 474.8 mM, which resulted in an increase of osmotic pressure to 1015 mOsm. Hypotonic stress was provided by decreasing the NaCl concentration.

At the time of the experiment the cell was illuminated with a fiberoptics light source to provide dim light. We assumed that such light level was similar to that experienced by the cells in their natural habitat. On the reef the plants were found on the underside of coral debris covering the shallows of the reef.

Cells were impaled and voltage-clamped by the two-electrode technique, and *I-V* curves obtained as described for experiments on *Chara* (Beilby, 1990). The cells were clamped to a bipolar staircase protocol generated by LSI 11/73 computer with pulses of 100 msec separated by 250 msec at the resting membrane potential difference (p.d.) level. The last 10 points of each membrane p.d. and current staircase pulse were averaged to form the *I/V* profile. The data-logging of each *I-V* scan took 8 sec. In later experiments the cell p.d. was monitored by a chartrecorder between the applications of the *I/V* protocol. The LSI 11/73 computer fitted polynomials to the *I/V* data segments, three data points at a time. The *G/V* profiles were calculated by differentiation of each polynomial segment. In later calculations performed by Mathematica 2.2.3, a single polynomial was fitted simultaneously to the whole *I/V* profile. The accuracy of the fitting procedure can be judged from Fig. 1*b*, which shows the average data points and standard errors. Further, the *G/V* profile obtained by differentiation of this polynomial was compared to that generated from segment fit by the LSI 11/73 computer to avoid artefacts. As two membranes in series were measured, it was instructive to generate *R/V* profiles, as two resistors in series are directly additive. However, the voltages across each membrane are not equal to the clamp voltage (*see* Discussion). $R(V)$ was obtained by reciprocal of the $G(V)$ polynomial.

The AC (alternating current) conductance was measured by clamping the cell to its resting p.d. with a small (5 to 10 mV) 5 Hz sine wave signal superimposed. The conductance was calculated as described in Beilby and Beilby (1983). This approach enabled us to measure the conductance of the membranes soon after impalement, when the conductance tended to be very high and the *I/V* curve protocol often caused irreversible damage.

The cells were held in a silver wire coil, which also constituted the current sink. The current-injecting electrode was made from a Pt/Ir wire, 30 μm in diameter, which has been broken under tension and heated to form a sharp point. The wire protruded from a tightly fitting glass micropipette by about 0.1 mm. The taper of the micropipette was very gradual and it was inserted far into the cell to position the wire tip in the center. We found that this rather thick wire was necessary to pierce the exceptionally tough cell wall of *Ventricaria*. The alternative strategy of using a broken-back glass micropipette to penetrate the cell wall and subsequently manipulating thinner wire into the cell seemed to cause more damage to the cell.

The cell wall was too tough and the cytoplasmic layer too narrow to insert electrodes into cytoplasm. The method of Davis (1981) of approaching the cytoplasm "through" the cell was tried, but the elec-

trodes blocked (or were excluded from the cytoplasm) too fast to perform an *I/V* scan. Our preliminary investigations suggest that the cytoplasm has an unusual spongelike structure, interpenetrated by the vacuole (Shepherd, M.J. Beilby, Cherry, and M.A. Bisson, *in preparation*). The structure studies of aplanospores and mature cells will enable us to develop techniques to make electrical contact with the cytoplasm.

In the meantime, however, the vacuolar impalement provides a lot of information about the system, such as the slow response of the *I/V* profiles to changes in $[K^+]_o$. The electrode in the vacuole almost never blocked and experiments could be performed for many hours.

Abbreviations:

ASW artificial seawater; E_K Equilibrium potential for K^+; E_{vo} vacuolar p.d.; E_{co} plasmalemma p.d.; E_{cv} tonoplast p.d.; E_p pump reversal p.d.; E_{leak} leak (background) current reversal p.d.; G_K conductance of K^+ channels; G_p pump conductance; G_{in} inward rectifier conductance; G_{out} outward rectifier conductance; G_{leak} leak (background) current conductance; G_{co} plasmalemma conductance; G_{cv} tonoplast conductance; *G/V* conductance-voltage; HGSS Hansen, Gradmann, Sanders, Slayman model; *I/V* Current-voltage; *I* clamp current; p.d. potential difference; R_{vo} resistance of plasmalemma and tonoplast in series; R_{co} plasmalemma resistance; R_{cv} tonoplast resistance; *R/V* resistance-voltage; S Siemen; SE standard error.

Results

Steady-state *I/V* Profiles as Function of $[K^+]_o$

The response of the resting p.d. as a function of $[K^+]_o$ is shown in Fig. 1*a* and the Table. The resting p.d. (and the *I/V* profile) took 20 min or more to stabilize in each solution. Only such stable values were used in the statistics. The average current-voltage profile in ASW is shown in Fig. 1*b* (dark violet). The *G/V* profile exhibited a maximum at ~+50 mV (near resting p.d., indicated by dashed vertical line) and a minimum near −100 mV (Fig. 1*c*, dark violet). A slope conductance, G_{slope}, was calculated by fitting a straight line to the data, between −25 and +75 mV (*see* Table). The Table also gives the AC conductance, G_{AC}, measured around the resting p.d. by imposing a sine wave (*see* Materials and Methods). The *R/V* profile (Fig. 1*d*, dark violet) displayed a striking peak at −100 mV.

As $[K^+]_o$ was decreased from 10 to 1 mM, the average resting p.d. stabilized at a more negative level (*see* Fig. 1*a* and Table). The shape of the *I/V* curve was quite different to that in ASW (Fig. 1*b*, green). Now the conductance maximum was seen at −100 mV, while the minimum occurred at +100 mV (Fig. 1*c*, green). The peak in the *R/V* profile has moved to p.d. of +100 mV (Fig. 1*d*, green). A similar behavior was observed at even lower $[K^+]_o$ of 0.1 mM (Fig. 1*b–d*, blue). For the average resting p.d. and slope conductance, *see* Table.

As $[K^+]_o$ was increased from 10 to 100 mM, the average resting p.d. became more positive (*see* Fig. 1*a* and Table). Surprisingly, the average conductance decreased compared to that in ASW and the *I/V* curve became nearly linear, except at extreme potentials (*see* Table and Fig. 1*b–d*, red). However, the *R/V* profile did show two small peaks.

Steady-state *I/V* Profiles as a Function of Osmotic Pressure

In response to hypertonic stress (25 mOsm), the cell resting p.d. became more positive. The mean value for the p.d. of cells responding to hypertonic stress is given in the Table. Although this is not significantly different from the value for the average control value reported above, not all experiments were performed on all cells, and the control values shifted somewhat during experiments. The average p.d. for matched controls (controls immediately before and after the hypertonic stress) and the average hyperpolarization in the 6 experiments is shown in the Table. It took an average of 80 ± 12 min for the cells to achieve the final steady value. This rather long period correlates well with turgor regulation (M.A. Bisson and M.J. Beilby, *in preparation*). The *I-V* curves were similar to those in ASW, but showed a more pronounced nonlinearity (Fig. 2*a*), with a higher conductance at positive potentials and a negative conductance region near −70 mV (Fig. 2*b*). Between 0 and ~−60 mV detailed analysis of the staircase current pulses showed a slow decay not reaching steady value by the end of the pulse. The current time dependence in this p.d. window will be further investigated, using long pulses of the order of seconds.

In response to hypotonic stress greater than 50 mOsm, the cells depolarized and adopted similar profiles to those observed in $[K^+]_o$ at and below 1.0 mM.

Time Dependence of the *I/V* Profiles

Recovery From Impalement Trauma

Immediately after impalement the cell resting p.d. was often negative and the conductance was very high; three values obtained by sine wave technique were 51, 107, and 132 S m^{-2}. The *I/V* curves obtained within the first hour after impalement showed several inflection points (Fig. 3*a*) with conductance displaying a local minimum near zero, with maxima on either side (Fig. 3*b*). In the *R/V* profile (Fig. 3*c*), these features become difficult to distinguish. The cells in such a high conductance state were more fragile and if changes in solution or voltage-

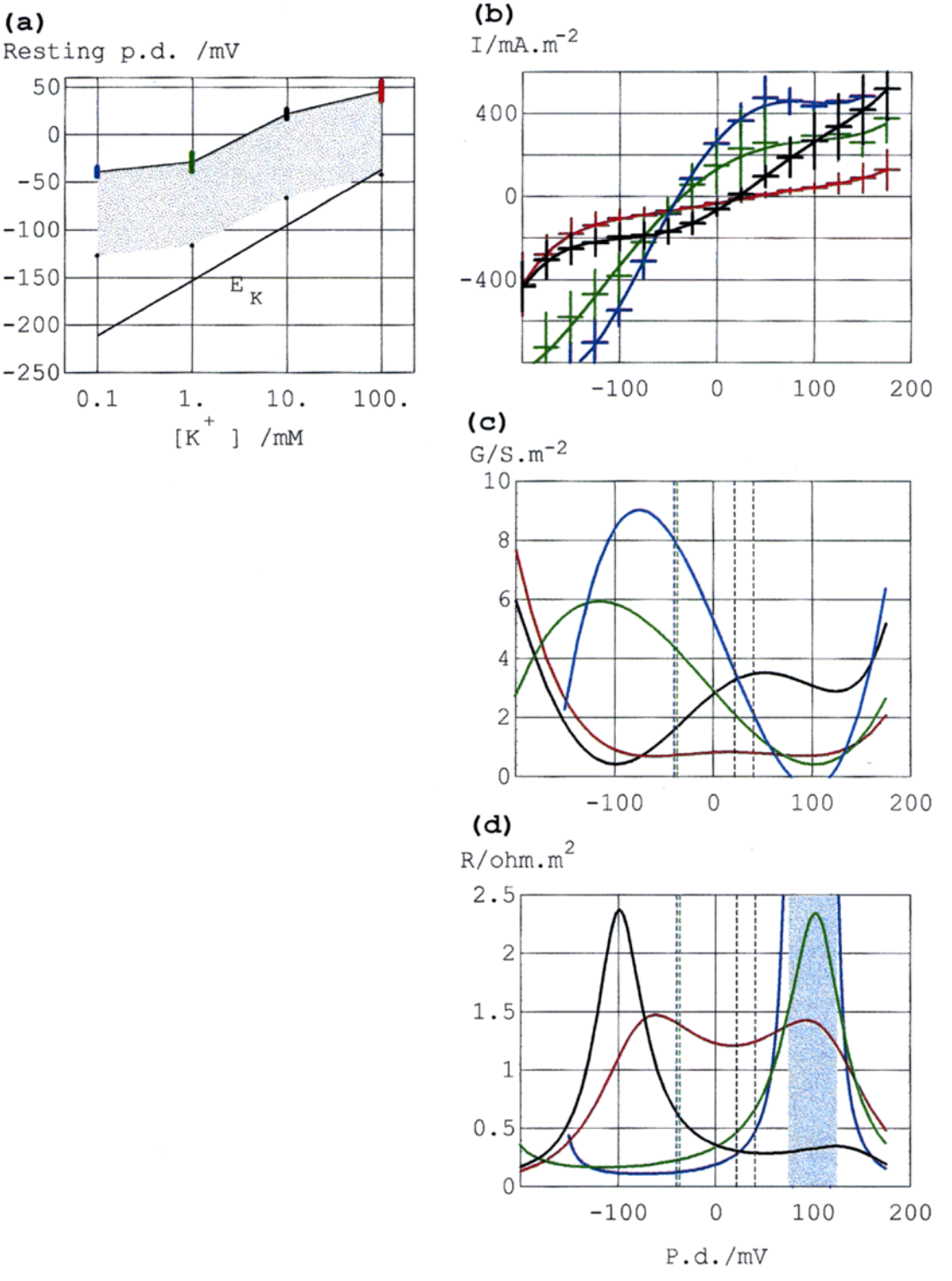

Fig. 1. **(a)** The resting vacuolar p.d. as function of $[K^+]_o$. Measurement from 6 to 16 cells (and several *I/V* profiles for some cells) are averaged for each point. The bars indicate standard error. The shaded band shows the projected resting p.d. across plasmalemma, assuming constant tonoplast potential of +88 mV (*see* text). The Nernst potential for K^+, E_K, across plasmalemma is plotted as continuous line, taking $[K^+]_{cyt}$ as 434 mM (*see* text).

The *I/V* (*b*), *G/V* (*c*) and *R/V* (*d*) profiles from 16 cells stabilized in ASW (10 mM K^+, dark violet); 9 cells stabilized in 1.0 mM K^+ medium (green); 6 cells stabilized in 0.1 mM K^+ medium (blue) and 9 cells stabilized in 100 mM K^+ medium (red). The data have been sorted into 25 mV bins indicated by horizontal bars. The vertical bars show the standard error. The *I/V* data were fitted with a polynomial, shown by the continuous line. The *G/V* profile was computed by differentiation. The *R/V* profile was obtained as reciprocal of the *G/V* profile. The shaded region signifies undefined and negative resistance. The dashed vertical lines in (*c*) and (*d*) indicate the resting p.d.

Table. Electrical parameters as function of $[K^+]_o$

$[K^+]_o$ mM	E_{vo} mV	ΔE mV	G_{slope} Sm^{-2}	R_{slope} Rm^2	G_{AC} Sm^{-2}
0.1	−39 ± 5 (6)		8.4 ± 1.7	0.12 ± 0.025	
1.0	−29 ± 11 (9)	10	5.0 ± 1.4	0.20 ± 0.050	
10.0 (ASW)	+21 ± 6 (16)	50	3.3 ± 0.9	0.30 ± 0.080	11.0 ± 6.7 (7)
100.0	+43 ± 10 (9)	22	0.83 ± 0.3	1.21 ± 0.450	
Hypertonic	+18 ± 8 (6)		5.0 ± 2.6	0.2 ± 0.110	
ASW control	+6 ± 5 (6)	−11 ± 7.7 (6)			

The results for the p.d. and G_{AC} are expressed as mean and standard error with the numbers of cells tested given in brackets. More than one measurement was often taken from each cell. The change in p.d., ΔE, gives the average change in p.d. from the previous medium. G_{slope} was calculated by fitting a straight line to the *I/V* data (Figs. 1*b* and 2*a*) passing through the resting p.d. The error was calculated from extreme lines that could be fitted within the error bars. R_{slope} was calculated as a reciprocal, with the same percentage error as in G_{slope}. The data obtained in hypertonic medium are included for comparison.

clamp experiments were performed at this time, they were less likely to survive. (Note, for instance, that *I/V* 2 displayed greater conductance than *I/V* 1 in Fig. 3*a* and *b*.) Consequently, the cells were allowed sufficient time after impalement (up to 5 hr) for the *I/V* profile to stabilize. In 5 out of 10 cells, oscillations in p.d. were observed at the time of recovery (Fig. 4*a*). The *I/V* characteristics (Fig. 4*b*) recorded at the crest and troughs of the oscillation show that the increasingly positive resting p.d. was reflected by an increase in conductance at positive clamp p.d.s and an appearance of negative conductance region at negative clamp p.d. (Fig. 4*c*).

Change in $[K^+]_o$

As $[K^+]_o$ was decreased from 10 to 1 mM, oscillations in p.d. were observed in 5 out of 6 cells (Fig. 5). The slow evolution of the low $[K^+]_o$ state (Fig. 1*b–d*, green) is shown in Fig. 6: the stable profile took 35 min to develop (*I/V* 3) and 29 min back in ASW to reverse (*I/V*s 4 and 5).

A typical time course for the change in conductance with time after transfer to high $[K^+]_o$ solution is shown for a single cell (Fig. 7). In this case, the conductance has flattened out over the course of 15 min (Fig. 7*b*). In other cases, the new conductance state was achieved in 5 min and remained stable. However, the *R/V* profile (Fig. 7*c*) shows that further increase of resistance occurred at 29 min (*I/V* 4). Note also that even after 66 min after the cell was returned to ASW, the *R/V* profile did not return to that seen in the control. The cells were more fragile in the high $[K^+]_o$ solution, and often died, if left in this solution for periods longer than 15 min.

Discussion

The Effect of $[K^+]_o$ on Steady-state *I/V* Characteristics

Plant systems amenable to *I/V* analysis, such as charophytes and guard cells, show Nernstian response to change in $[K^+]_o$ from ~1 mM to higher concentrations. The K^+ channel *I/V* profiles are linear near reversal p.d. (close to E_K), but show negative conductance regions resulting from fast channel closure, as the p.d. is clamped beyond some critical level in both a positive and negative direction (e.g., Beilby, 1985; Blatt, 1988). In charophytes the plasmalemma conductance increases considerably in high $[K^+]_o$, but the plasmalemma *I/V* characteristics remain dominant when both membranes are voltage-clamped in series (Beilby, 1990). The exposure of *Ventricaria ventricosa* to change in $[K^+]_o$ reveals a very different behavior on several levels. The Table and Fig. 1*a* indicate, that while E_{vo} moves in the right direction with $[K^+]_o$ increase, the conductance decreases (or resistance increases). Similar trends were observed by Asai and Kishimoto (1975) for *Valonia aegagropila* and Findlay et al. (1971) for *Chaetomorpha darwinii*, but, surprisingly, not by Davis (1981) for *Valonia* (*Ventricaria*) *ventricosa*. While the *I/V* profile in ASW (Fig. 1*b–d*, dark violet) features conductance maximum near resting p.d., which is not unlike the K^+ state of charophytes (Beilby, 1985), it evolves into a very unusual profile for $[K^+]_o$ between 1.0 and 0.1 mM (Fig. 1*b–d*, blue and green). The conductance increases (resistance decreases) in the negative region and peaks negative to the resting p.d. level. In the high $[K^+]_o$, on the other hand, the *I/V* profile becomes close to linear in the vicinity of the resting p.d. and the conductance drops (resistance rises) considerably (Fig. 1*b–d*, red).

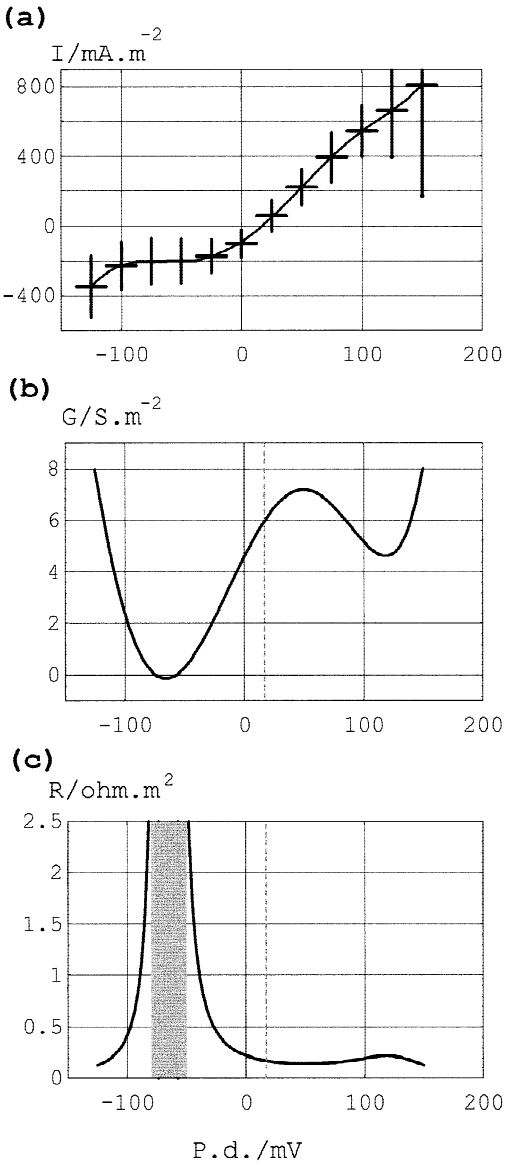

Fig. 2. The *I/V* (*a*), *G/V* (*b*) and *R/V* (*c*) profiles from 6 cells stabilized in hypertonic solution (*see* Materials and Methods). The data have been treated as in Fig. 1.

The AC conductance, G_{AC}, is significantly higher than G_{slope} or the conductance in Fig. 1*b* (dark violet), suggesting a different frequency dispersion of the *Ventricaria* cell wall/cytoplasm/membranes system to that of the charophytes, where the frequency of 5 Hz delivers primarily membrane conductance (Beilby, 1990).

Analysis of the Time Dependence of the *I/V* Profiles

In charophyte plasmalemma the response to changes in $[K^+]_o$ is fast (seconds), once the K^+ channels are open

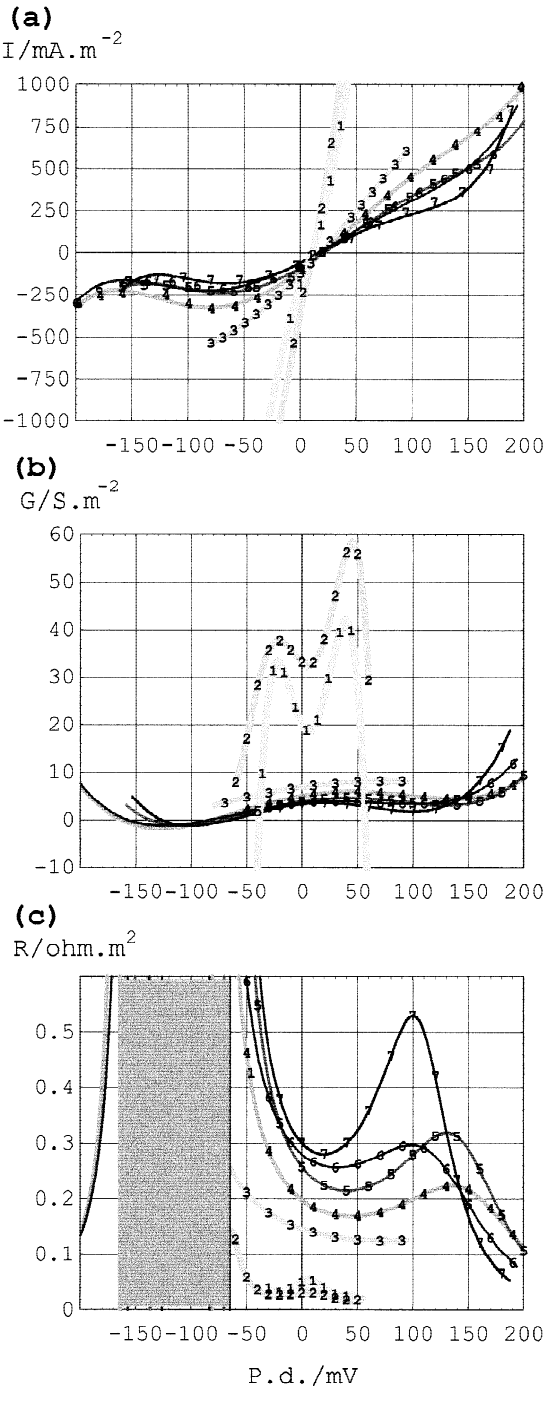

Fig. 3. The *I/V* (*a*), *G/V* (*b*) and *R/V* (*c*) profiles of a cell as a function of time after impalement. In (*a*) the data points have been replaced by numbers. The *I/V* data were fitted with polynomials, as shown by continuous lines. The thickness of the lines decreases as a function of time after impalement, while the gray level increases. *I/V*(1) was obtained 32 min after impalement, *I/V*(2) 57 min, *I/V*(3) 75 min, *I/V*(4) 105 min, *I/V*(5) 115 min, *I/V*(6) 125 min and *I/V*(7) 130 min. In (*b*) and (*c*) the numbers are superimposed on the continuous profiles at arbitrary intervals. The undefined resistance is shown by gray shading.

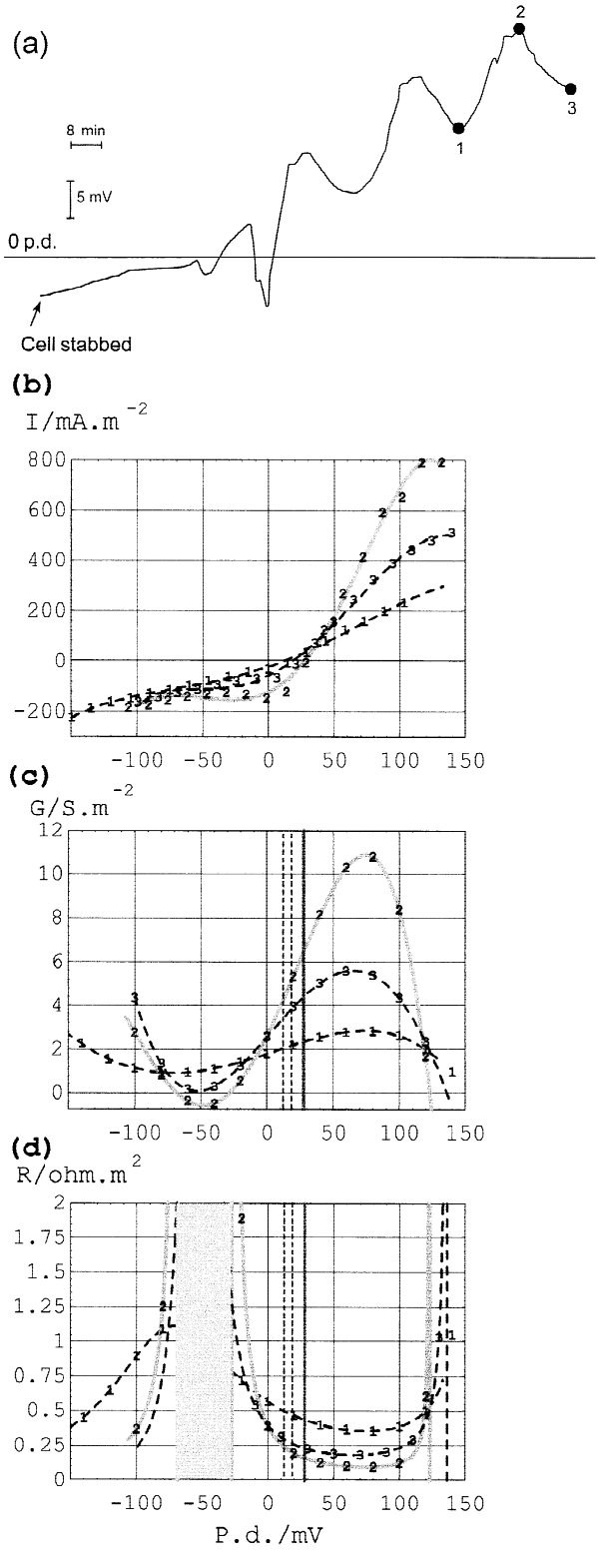

Fig. 4. Oscillations of vacuolar p.d. after cell impalement (*a*) and *I/V* (*b*), *G/V* (*c*) and *R/V* (*d*) profiles at the crest and trough of oscillation, as shown by dots in (*a*).

(Beilby, 1985). If the K^+ channels of the *Ventricaria* plasmalemma behave similarly, then any prompt changes in conductance following outside concentration change should be due to plasmalemma response. Whether the change in $[K^+]_o$ is communicated to the tonoplast by corresponding change of K^+ concentration in the cytoplasm or by some other messenger, the response of the tonoplast transporters is expected to take some minutes. The slow evolution of the *I/V* profiles following both decrease and increase of $[K^+]_o$ suggest that we mainly observe changes in tonoplast transporters (Figs. 6 and 7, respectively), the plasmalemma being too conductive to contribute substantially to *G/V* or *R/V* profiles. This view is supported by the data from *Chaetomorpha*, where R_{co} drops with increasing $[K^+]_o$ (Findlay et al., 1971). The effect of high $[K^+]_o$ on the tonoplast transporters (or the increase of K^+ concentration in the cytoplasm) seems to persist, as the *R/V* profile does not return to that of normal ASW even after some hours (*see* Fig. 7). Persistent changes in R_{vo} and E_{vo} $[K^+]_o$-dependence was also observed by Asai and Kishimoto (1975), after pretreating *Valonia aegagropila* in 100 mM K^+. We interpret the high K^+ *I/V* profile as describing the tonoplast with the pump affected by the high $[K^+]_o$.

Charophyte plasmalemma K^+ channels close promptly once $[K^+]_o$ drops below ~1 mM and the *I/V* profiles become almost linear with a low conductance (Beilby, 1985). However, *Ventricaria I/V* profiles display high conductance regions at negative p.d.s (*see* Fig. 1*b–d*). The conductance increases even further as $[K^+]_o$ diminishes to 0.1 mM. Once again, these *I/V* profiles develop over minutes implicating changes of the transporter kinetics at the tonoplast. The same type of profile can be observed if the cells are exposed to hypotonic shock of more than ~50 mOsm/kg (M.J. Bisson and M.A. Beilby, *in preparation*). Guggino and Gutknecht (1982) subjected *Valonia macrophysa* to hypo-osmotic shock and showed that turgor regulation was completed within hours by decreases of K^+, Cl^- and Na^+ in the vacuole. At the time of regulation the E_{vo} moved to negative region from −40 to −70 mV. Guggino and Gutknecht (1982) suggested an inhibition of the pump, while Zimmermann and Steudle (1974) postulated reversal of the pump. As the conductance is high (resistance is low) near the resting p.d., there must be a high conductance elements at both membranes (*see* Fig. 1*c* and *d*). While it is difficult to imagine the pump working in reverse, perhaps the pump is short-circuited by an increasing background current of mainly K^+ and Cl^-. The high conductance at the plasmalemma suggests that *Ventricaria* K^+ channels may have a lower concentration trigger for closing than those of charophytes. Thus we associate the low $[K^+]_o$ profile with the "pump off" or pump being short-circuited by other transporters at p.d.s more negative than +50 mV. It also seems that the signal for hy-

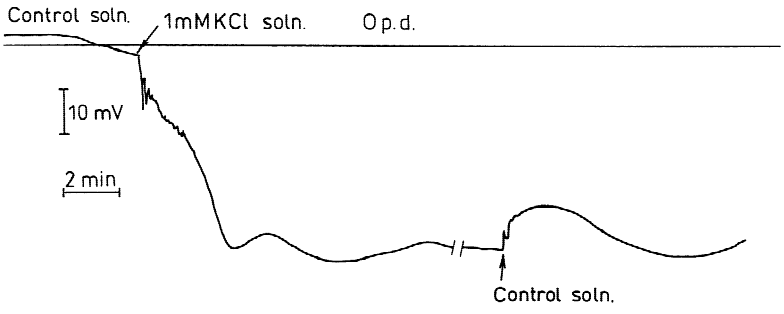

Fig. 5. Oscillations of the vacuolar p.d. as the medium is changed from ASW to low K^+ soln (1.0 mM) and back to ASW.

potonic turgor regulation may be decrease of K^+ concentration in the cytoplasm. This hypothesis is under further investigation.

The *I/V* profiles at the time of recovery show high conductance throughout the accessible p.d. window in the first hour after impalement (Fig. 3, profiles 1 and 2). The complex *G/V* profiles suggest that this is not due to general leakage through the damaged membranes around the electrodes, as constant conductance would be likely, at least near the reversal p.d. level. Further, the turgor pressure recovery occurs on faster time scale (M.A. Bisson and M.J. Beilby, *in preparation*). At this high conductance, the contribution of the plasmalemma is likely to be more visible. In Fig. 4*a* the resting p.d. is gradually becoming more positive after impalement. At the crest of the oscillation, the *I/V* profiles (Fig. 4*b–d*) become similar to those obtained in hypertonic solution (Fig. 2), where Gutknecht (1967) observed stimulation in both K^+ influx and inward short-circuit current. Consequently, we associate this *I/V* profile with the pump working hard during recovery or hypertonic turgor regulation.

The oscillations in membrane p.d. were also observed, as $[K^+]_o$ was changed (Fig. 5), indicating presence of a feedback loop or an interaction of two regulatory mechanisms.

Model

Figure 8 outlines the proposed model circuit of the two membranes in series. Davis (1981) showed that the p.d. of the plasmalemma alone is dominated by K^+ conductance, even if the response to $[K^+]_o$ is not fully Nernstian, especially at low concentrations. Such behavior is seen in most plant cells and is consistent with the Goldman model, where permeability to other ions (Cl^- and Na^+) becomes more important at low $[K^+]_o$. As we did not measure cytoplasmic and vacuolar concentrations of the major ions at the time of the experiment, we simulate the *I/V* profile of the plasmalemma by a constant conductance K^+ transporter with a constant conductance "leak" or "background" current subsumed at low $[K^+]_o$. We plan to measure concentrations of major ions in the compartments and the Goldman equation will then be incorporated into the model.

The inward and outward rectifiers are observed in the vacuolar *I/V* profiles (Fig. 1*b–d*) and are present, therefore, at both membranes.

The tonoplast contains the unknown pump, which is responsible for the large positive p.d. (Gutknecht, 1966; Davis, 1981), the leak (background) current of unknown composition (probably K^+ and Cl^-) and rectifiers. For $I = 0$, the E_{co} approaches E_K, E_{vc} moves between E_p and E_{leak} depending on the pump activity.

At the time of the voltage clamp, current I flows in either direction in the course of the bipolar staircase command. The p.d.s E_{vo}, E_{co} and E_{cv} are related to the circuit elements as shown below:

$$G_{co} = G_K + G_{out} + G_{in} \quad (1)$$

$$R_{co} = 1/G_{co} \quad (2)$$

$$G_{cv} = G_p + G_{leak} + G_{out} + G_{in} \quad (3)$$

$$R_{cv} = 1/G_{cv} \quad (4)$$

$$R_{vo} = R_{co} + R_{cv} \quad (5)$$

$$E_{vo} = IR_{co} + IR_{cv} \quad (6)$$

From Eq. (6), it is apparent that the clamp p.d. distributes itself according to ratio of R_{co} and R_{cv}. For instance, for R_{cv} five times R_{co} (Davis, 1981), E_{vo} change of 50 mV will result in E_{cv} change of 40 mV and E_{co} change of 10 mV. The situation is further complicated by the circuit elements being voltage dependent. While R_{co} and R_{cv} are directly additive (Eq. 5) and the *R/V* profiles might be the easiest to interpret than the *G/V* profiles, the p.d. across each membrane is not the same as the clamp p.d. level. Consequently, the features (such as the prominent peaks) in the *R/V* profiles (Fig. 1*d*) are only approximate in their shape and location.

Testing various forms of p.d.-dependence of the circuit elements of the model (Fig. 8) facilitates interpretation of the data, as well as suggesting future experiments. The high $[K^+]_o$ data set provides a good starting point, as it is very likely that the plasmalemma is highly conductive under such conditions and the *R/V* profile reflects the electrophysiology of the tonoplast. The outcome can be seen in Fig. 9. The rectifiers at both membranes were simulated by exponential functions similar to those used for *Chara* by Beilby and Walker (1996). G_K (plasma-

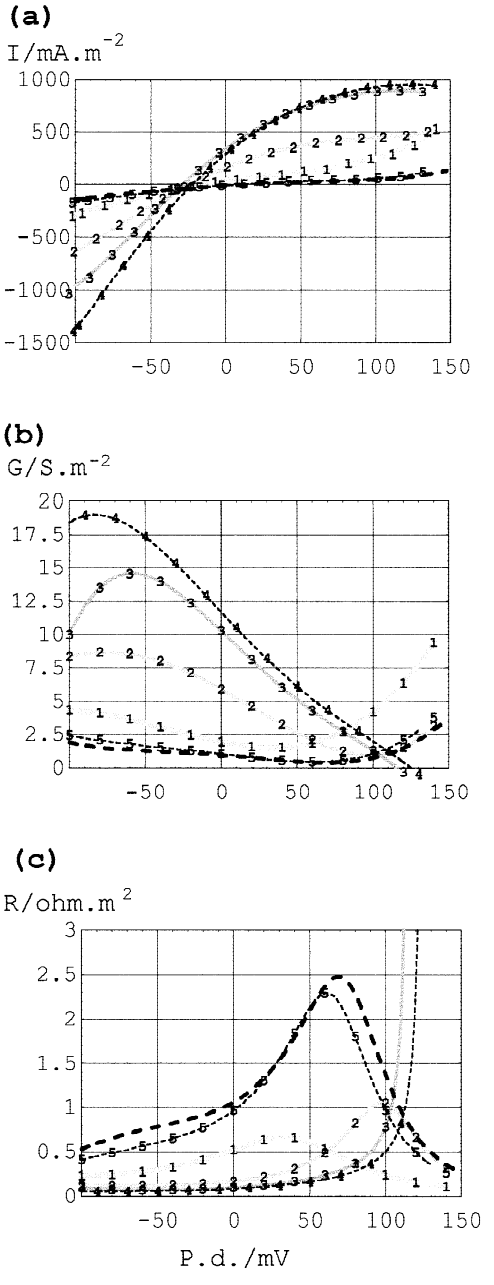

Fig. 6. Sequence of *I/V* (*a*), *G/V* (*b*) and *R/V* (*c*) profiles after the cell was exposed to low K^+ (1.0 mM) solution. The *I/V* data were fitted with polynomials, as shown by continuous lines (low K^+) and dashed lines (ASW). The thickness of the continuous lines decreases as a function of time after solution change, while the gray level increases. *G/V* and *R/V* profiles were calculated as in Fig. 1. The control *I/V* (dashed thick line, un-numbered) was obtained 45 min after the cell was stabilized in ASW. The *R/V* profile does not show the sharp peak at −100 mV typical of ASW, as it had been exposed to 100 mM K^+ in the early part of the experiment. However, the trend in low K^+ solution was typical, when compared to other experiments without the high K^+ exposure. The *I/V*(1) was taken after 7 min in low K^+, *I/V*(2) 17 min in low K^+, *I/V*(3) 25 min in low K^+, *I/V*(4, dashed) 3 min back in ASW and *I/V*(5, dashed) 29 min in ASW. In (*b*) and (*c*) the continuous lines are identified by the same numbers at arbitrary intervals.

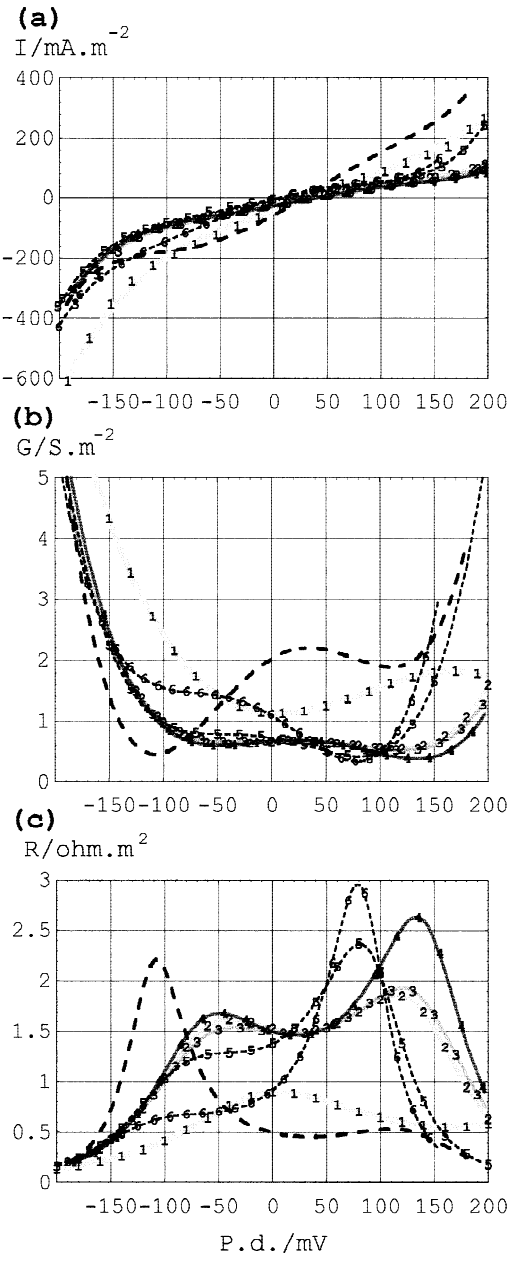

Fig. 7. Sequence of *I/V* (*a*), *G/V* (*b*) and *R/V* (*c*) profiles after the cell was exposed to high K^+ (100 mM) solution. The *I/V* data were treated as in Fig. 6. The control *I/V* (dashed thick line, un-numbered) was obtained after the cell was stabilized in ASW 2 hr 22 min after impalement, *I/V*(1) 4 min in high K^+, *I/V*(2) 16 min in high K^+, *I/V*(3) 24 min in high K^+, *I/V*(4) 29 min in high K^+ and *I/V*(5, dashed) 2 min back in ASW and *I/V*(6, dashed) 66 min back in ASW. In (*b*) and (*c*) the continuous lines are identified by the same numbers at arbitrary intervals.

lemma) and G_{leak} (tonoplast) were made p.d. independent (in absence of any data) with magnitudes resulting in G_{co} (near resting p.d.) about five times greater than G_{vc} (*see* Fig. 9*b* and *d*), as suggested by early recovery *R/V* profiles (Fig. 3*d*, profiles 1 and 2).

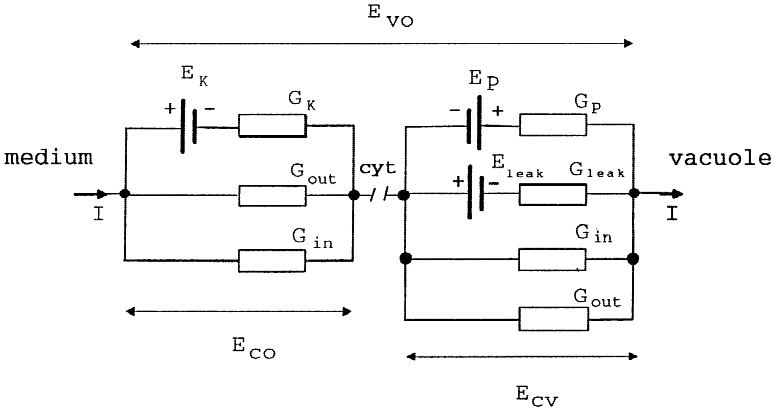

Fig. 8. The equivalent circuit for the plasmalemma and tonoplast in series. The electrical characteristics of the plasmalemma are approximated by the conductance of K^+ channels, G_K, and inward and outward rectifiers, G_{in} and G_{out}, respectively. The leakage conductance is assumed to be small compared to K^+ conductance at high $[K^+]_o$ and subsumed in G_K at low $[K^+]_o$. The electrical characteristics of the tonoplast are approximated by G_{pump}, the rectifiers, G_{in} and G_{out}, and a leakage conductance G_{leak}. If the clamp current, I, across the circuit reduces to 0, the p.d. across the plasmalemma approaches E_K and the p.d. across the tonoplast approaches some value intermediate between E_{leak} and E_{pump}. The relationships among some of the elements are given in the text.

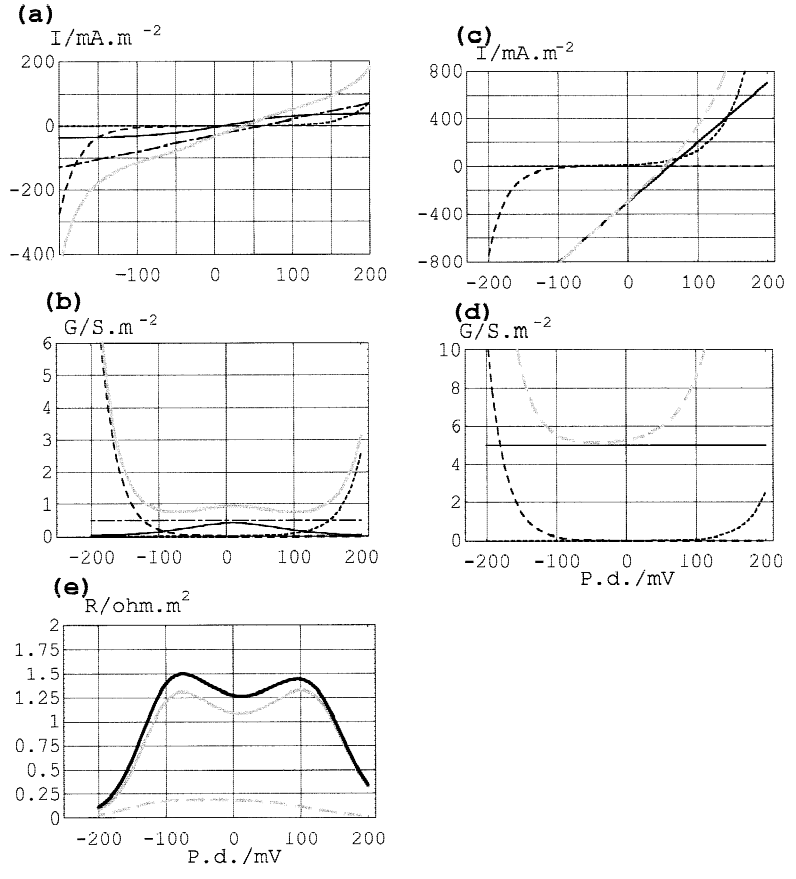

Fig. 9. The *I/V* characteristics of model tonoplast (*a*) and plasmalemma (*c*) in high $[K^+]_o$. The rectifiers (thin dashed lines) in each case are described by exponential functions as in Beilby and Walker (1996). The pump (thin continuous line) is simulated by a two-state HGSS model (Hansen et al., 1981). Note that the pump current is inward, as expected for an inflow of positive charge into the vacuole. The leak (background) current (unequal dashed line) was assigned E_{leak} close to zero, near E_K for the tonoplast. The total current is shown as a thick gray line. The plasmalemma characteristics are dominated by the K^+ conductance, which was set to be constant with p.d., in absence of more information. E_K for the plasmalemma has been set for high $[K^+]_o$ near −40 mV. The total current is shown as dashed thick gray line. The conductances for the tonoplast, G_{cv}, (*b*) and plasmalemma, G_{co}, (*d*) relate to the circuit in Fig. 8. The total resistance of the tonoplast, R_{vc}, and plasmalemma, R_{co}, are added in (*e*) and shown as thick black line.

The pump *I/V* characteristics were simulated by the HGSS two-state model (Hansen et al., 1981), with parameters manipulated to obtain conductance maximum near zero. Taking energy supplied by ATP as 30.56 kJ/mol and K^+ concentrations in vacuole and cytoplasm as measured by Gutknecht (1966), the reversal p.d. for the pump, E_p, was calculated as +300 mV for 1 K^+/ATP transported or +150 mV for 2K^+/ATP transported. Davis, Hunt and Sanders (1994) found that H^+ pumping vacuolar ATPases have a variable stoichiometry. If *Ventricaria* pump behaves similarly, E_p is likely to be in the range of +100 to +300 mV. The E_p in the model was adjusted to ~+200 mV (Fig. 9*a*, thin continuous line). Without extensive manipulation, a striking similarity of the R_{vo}/V profile (Fig. 9*e*) was obtained to the high $[K^+]_o$ data in Fig. 1*d* (red).

The modeling of the data in lower $[K^+]_o$ was not attempted at this point, as the plasmalemma transporters might contribute more to the total *R/V* profile. However, some insight into the system was gained by curve-fitting

the high K^+ data set. Rather than associating the prominent resistance peaks at −100 and +100 mV (Figs. 1*d*) with the closure of the K^+ channels on the plasmalemma, the slow development of this feature with cell recovery (Fig. 4) or change of $[K^+]_o$ suggests that it might reflect the constant current region of the K^+ pump at the tonoplast (*see* Fig. 9). At p.d.s, where the pump current is constant, the resistance of the tonoplast approaches the resistance due to the leak (background) pathway. If the p.d. is then stepped in further negative or positive direction, the resistance drops due to activation of the negative or the positive rectifier.

In conclusion, we have shown that the membranes of *Ventricaria* respond very differently to change of $[K^+]_o$ from 0.1 to 100 mM as compared to most plant cells. The *I/V* (*R/V*) analysis supports the earlier hypothesis of Gutknect (1967), that a K^+ pump is operating at the tonoplast. A detailed modeling of this novel pump was not attempted at this stage, as it will be necessary to isolate the *I/V* characteristics of the tonoplast. We plan to achieve this aim by obtaining the plasmalemma *I/V* alone from the avacuolate aplanospores and subtract it from the series *I/V* profile at constant current (Beilby, 1984).

The authors gratefully acknowledge Travel Grant from National Science Foundation (MAB) and Small Australian Research Council Grant (MJB). We thank the Great Barrier Reef Marine Park Authority for permission to collect *Ventricaria* and to Heron Island Research Station staff for great support while collecting cells. We would also like to thank the referees for their detailed and informative comments.

References

Asai, K., Kishimoto, U. 1975. Effects of sodium, potassium and chloride ions on the membrane potential of *Valonia aegagropila. Plant and Cell Physiol.* **16:**93–100

Beilby, M.J. 1984. Current-voltage characteristics of the proton pump at *Chara* plasmalemma: I. pH dependence. *J. Membrane Biol.* **81:**113–125

Beilby, M.J. 1985. Potassium channels at *Chara* plasmalemma. *J. Exp. Bot.* **36:**228–239

Beilby, M.J. 1990. Current-voltage curves for plant membrane studies: a critical analysis of the method. *J. Exp. Bot.* **41:**165–182

Beilby, M.J., Beilby, B.N. 1983. Potential dependence of the admittance of *Chara* plasmalemma. *J. Membrane Biol.* **74:**229–235

Beilby, M.J., Walker, N.A. 1996. Modeling the current-voltage characteristics of *Chara* membranes: I. The effect of ATP removal and zero turgor. *J. Membrane Biol.* **149:**89–101

Blatt, M.R. 1988. Potassium-dependent, bipolar gating of K^+ channels in guard cells. *J. Membrane Biol.* **102:**235–246

Blinks, L.R. 1929. Resistance and potential measurements across the protoplasm of *Valonia ventricosa. Carnegie Inst Wash., Year Book* **28:**277–179

Damon, E.B. 1930. Dissimilarity of inner and outer protoplasmic surfaces in *Valonia. J. Gen. Physiol.* **13:**207–221

Davies, J.M., Hunt, I., Sanders, D. 1994. Vacuolar H^+-pumping ATPase variable transport coupling ratio controlled by pH. *Proc. Natl. Acad. Sci. USA* **91:**8547–8551

Davis, R.F. 1981.Electrical properties of the plasmalemma and tonoplast in *Valonia ventricosa. Plant. Physiol.* **67:**825–831

Findlay, G.P., Hope, A.B., Pitman, M.G., Smith, F.A., Walker, N.A. 1971. Ionic relations of marine algae: III. *Chaetomorpha:* Membrane electrical properties and chloride fluxes. *Aust. J. Biol. Sci.* **24:**731–745

Findlay, G.P., Hope, A.B., Pitman, M.G., Smith, F.A., Walker, N.A. 1978. Ionic relations of marine alga *Valoniopsis pachynema. Aust. J. Plant. Physiol.* **5:**675–686

Guggino, S., Gutknecht, J. 1982. Turgor regulation in *Valonia macrophysa* following acute osmotic shock. *J. Membrane Biol.* **67:**155–164

Gutknecht, J. 1966. Sodium, potassium, and chloride transport and membrane potentials in *Valonia ventricosa. Biol. Bull.* **130:**331–344

Gutknecht, J. 1967. Ion fluxes and short-circuit current in internally perfused cells of *Valonia ventricosa. J. Gen. Physiol.* **50:**1831–1834

Hansen, U.-P., Gradmann, D., Sanders, D., Slayman, C.L. 1981. Interpretation of current-voltage relationships for "active" ion transport systems: I. Steady-state reaction-kinetic analysis of class-I mechanisms. *J. Membrane Biol.* **63:**165–190

Hastings, D.F., Gutknecht, J. 1974. Turgor pressure regulation: Modulation of active potassium transport by hydrostatic pressure gradients. *In:* pp. 79–83. Membrane Transport in Plants. U. Zimmermann and J. Dainty, editors. Springer, New York

Hastings, D.F., Gutknecht, J. 1975. Ionic relations and the regulation of turgor pressure in the marine alga, *Valonia macrophysa. J. Membrane Biol.* **28:**263–275

Olsen, J.L., West, J.A. 1988. *Ventricaria* (Siphonocladales-Cladophorales complex, Chlorophyta), a new genus for *Valonia ventricosa. Phycologia* **27:**103–108

Wang, J., Benz, R., Zimmermann, U. 1995. Effects of light and inhibitors of ATP-synthesis on the chloride carrier of the alga *Valonia utricularis:* is the carrier a chloride pump? *Biochem. Biophys. Acta* **1233:**185–197

Zimmermann, U., Steudle, E. 1974. The pressure dependence of the hydraulic conductivity, the membrane resistance and membrane potential during turgor pressure regulation in *Valonia utricularis. J. Membrane Biol.* **16:**331–352